


Numerical simulation of heat sinks with different configurations for high power LED thermal management

Thangamani Ramesh¹, Ayyappan Susila Praveen^{1,*}, Praveen Bhaskaran Pillai², and Sachin Salunkhe¹ 

¹ Department of Mechanical Engineering, Vel Tech Rangarajan Dr. Sagunthala R&D Institute of Science and Technology, Chennai 600062, Tamil Nadu, India

² Clean Energy Research Group, Department of Mechanical and Aeronautical Engineering, University of Pretoria, Pretoria 0002, South Africa

Received: 16 March 2022 / Accepted: 8 June 2022

Abstract. This study performed a steady-state numerical analysis to understand the temperature in different heat sink configurations for LED applications. Seven heat sink configurations named R, H-6, H-8, H-10, C, C3, and C3E3 were considered. Parameters like input power, number of fins, heat sink configuration were varied, and their influence on LED temperature distribution, heat sink thermal resistance and thermal interface material temperature were studied. The results showed that the temperature distribution of the H-6 heat sink decreased by 46.30% compared with the Cheat sink for an input power of 16 W. The result of the H-6 heat sink shows that the heat sink thermal resistance was decreased by 73.91% compared with the Cheat sink at 16 W. The lowest interface material temperature of 54.11 °C was achieved by the H-6 heat sink when the input power was used 16 W. The H-6 heat sink exhibited better performance due to more surface area with several fins than other heat sinks.

Keywords: LED / thermal resistance / FEA / heat sinks / temperature of interface material

1 Introduction

High-power LED is a semiconductor used for lighting indoor, outdoor, streets and automotive systems. LEDs have several advantages compared to traditional lighting systems, such as being environmentally friendly, high luminous efficacy (136 lm/W) [1], low radiated heat and long life (30,000–50,000 hours) [2]. However, only 20% of the electrical energy supplied to the LED is converted into visible light. The remaining electrical energy is transformed into waste heat [3]. Relatively high heat energy is accumulated within the small volume of the LED module. The heat flux is near 100 W/cm² for a small chip area [4]. This, in turn, reduces the LED's working lifespan and illumination potential [5]. The maximum temperature at the junction of the LEDs should be below 125 °C. Suitable cooling techniques can be used to extend the life and improve the operating efficiency of the LED. Therefore, the effectiveness of thermal management is a critical requirement for an LED lighting system. Typically, passive and active cooling techniques are used for LED cooling [6]. Active cooling is more expensive than passive cooling.

Moreover, passive cooling does not have any external moving parts [7]. Many studies focused on the various patterns of passive heat sinks for effective heat dissipation [8–12]. Li and Byon [13] experimentally and numerically explored the performance of radial finned heat sink with rectangular fins, rounded base and concentric ring at three different orientations (0°, 90° and 180°) for downlight application. Concentric ring fins of the radial heat sink with 90° orientation showed an improved heat transfer rate compared to the 180° orientation heat sink. Feng et al. [14] studied the free convection heat transfer through cross fin heat sink and plate-fins in a horizontal orientation. They observed that convective heat transfer performance of cross fin heat sink improved up to 15%. He et al. [4] used the finite element method to evaluate the thermal performance of LED chips based on the cold spray method. They concluded that using the copper substrate LED chip with cold spray solder method was improved heat transfer rate compared to the aluminium substrate LED chip. Abdelmlek et al. [2] numerically investigated the junction temperature, light output and lift time of LED package. A comparison of both LED chips mounted on a single substrate and individual substrate. They observed that using separated substrates rather than continuous ones reduces junction temperature by 14.38 percent, improves

* e-mail: drsalunkhesachin@veltech.edu.in

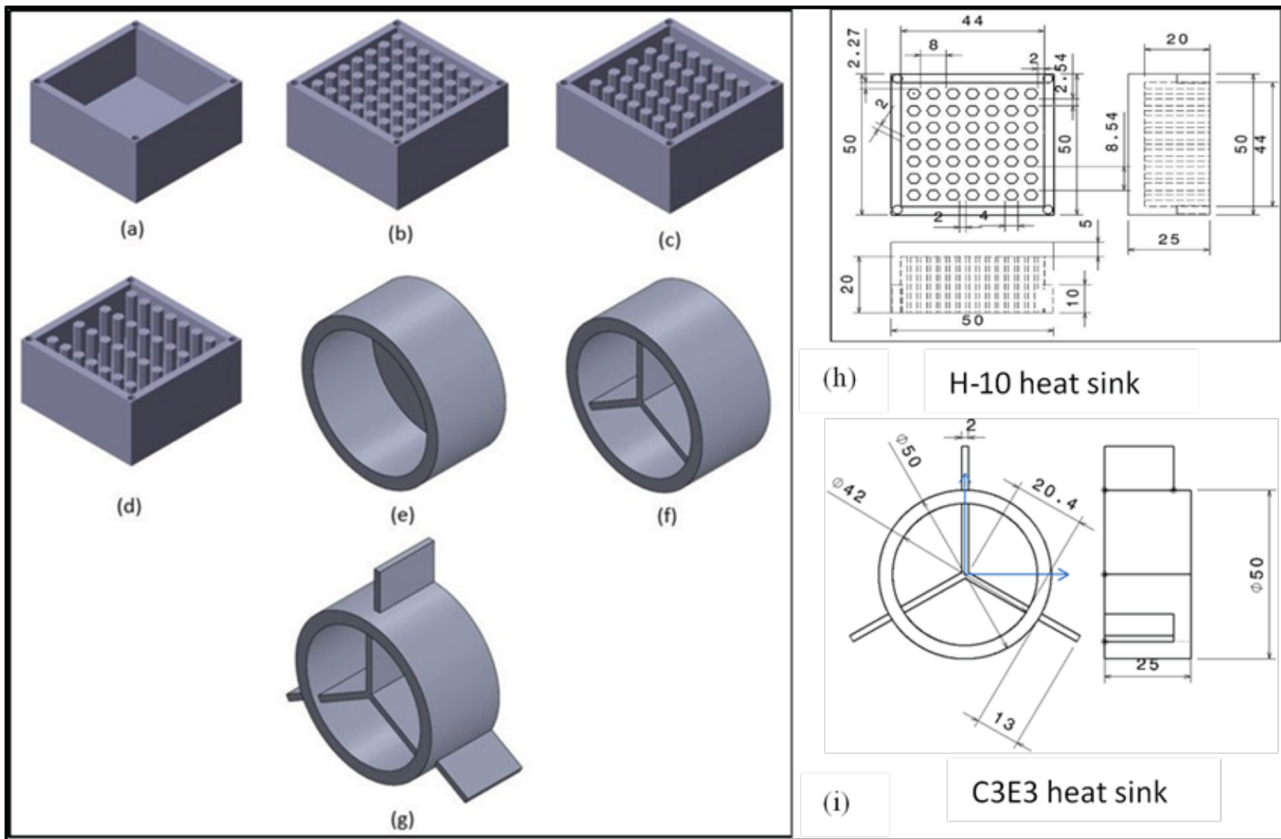


Fig. 1. Different heat sink configuration considered in this study (a) R (b) H-6 (c) H-8 (d) H-10 (e) C (f) C-3 and (g) C3E3 and heat sink dimension of (h) H-10 and (i) C3E3.

light output by 11.82 percent, and increases LED lifetime by 105212 hours. Jeong et al. [15] numerically studied using a horizontal fin heat sink with an opening model for LED application. The present study studied the thermal performance of high power LED with different configuration heat sinks using finite element simulation software. For this purpose, seven different configurations of heat sinks (R, H-6, H-8, H-10, C, C-3 and C3E3) were considered. The system's performance was evaluated with the temperature distribution, heat sink thermal resistance and thermal interface material temperature.

2 Numerical method

2.1 Heat sink geometry

Figure 1 shows the seven different configurations of the heat sink models considered for this study. The heat sink material is aluminium alloy 6063. The heat sinks are characterized by fin shape and the number of fins. Each heat sink was tagged as a heat sink without fin (R) (Fig. 1a) and a heat sink with a hexagonal fin having a pitch (pitch = latitudinal remoteness between the mid-point of a pin and adjacent fin). 6 mm (H-6) (Fig. 1b), 8 mm (H-8) (Fig. 1c), 10 mm (H-10) (Fig. 1d), radial heat sink without fin (C) (Fig. 1e), radial heat sink with three internal cavities (C-3) (Fig. 1f) and radial heat sink with

three internal cavity and three external fins (C3E3) (Fig. 1g). The fins in H-6, H-8 and H-10 heat sink 49, 35 and 28, respectively, and the fin dimension is 2×20 (side length \times height) used in the current study. In the case of the circular heat sink, the outer diameter, fin height, fin thickness, length of the external fin (from the outer surface), and inner diameter are 50 mm, 20 mm, 2 mm, 13 mm, and 42 mm respectively. In this study, four different input power was considered, i.e., 4 W, 8 W, 12 W and 16 W and corresponding internal heat generation is $11.19 \times 10^6 \text{ W/m}^3$, $22.38 \times 10^6 \text{ W/m}^3$, $33.57 \times 10^6 \text{ W/m}^3$ and $44.76 \times 10^6 \text{ W/m}^3$, respectively. Internal heat generation (heat source as LED module) occurred at the bottom surface of the heat sinks. SolidWorks version 2018 design software was used to design the heat sinks. Finite element simulation software ANSYS 17.2 was used to study the heat dissipation of heat sink fitted with LED module, and the maximum temperature value was identified.

2.2 LED package

In the present study, the working area of the LED module is $19 \times 19 \text{ mm}^2$. The thermal interface material is placed between the LED module and the bottom surface of heat sinks to reduce the LED module's thermal resistance (TIM), as shown in Figure 2. The thermal conductivity of

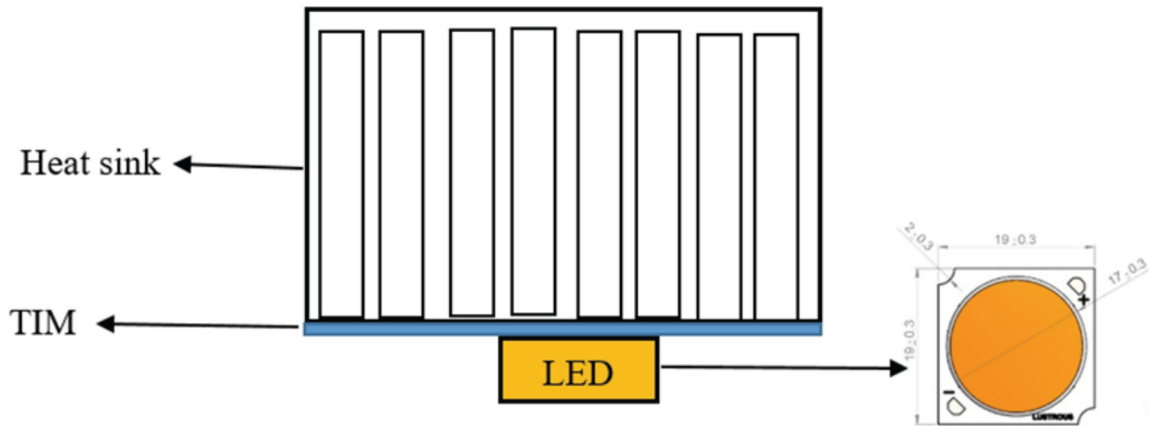


Fig. 2. Schematic representation of LED package with heat sink.

the heat sink, TIM and LED module is $202 \text{ W/m}^\circ\text{C}$, $1.9 \text{ W/m}^\circ\text{C}$ and $130 \text{ W/m}^\circ\text{C}$, respectively. The LED module's thickness and TIM are $990 \mu\text{m}$ and $50 \mu\text{m}$, respectively.

2.3 Assumptions and governing equations

In this study, the following assumptions were used to simulate steady-state conduction [2]:

- The steady-state conduction was relevant
- The materials of the model is homogeneous, isotropic, and temperature independent.

The governing equation is given in equation (1).

$$\frac{\partial^2 T}{\partial^2 x} k_x + \frac{\partial^2 T}{\partial^2 y} k_y + \frac{\partial^2 T}{\partial^2 z} k_z + Q = 0 \quad (1)$$

Where T is the temperature, Q is the heat flow from LED module and k_x , k_y and k_z refer to the thermal conductivity of material on X , Y , and Z directions.

2.4 Boundary conditions

- Constant film coefficient convection is 13 W/mK was applied to heat sink ambient temperature is 30°C [2].
- Power input (4 W , 8 W , 12 W and 16 W) to LED module as considered internal heat generation (W/m^3). The volume of LED module is $(1.9 \times 10^{-2} \times 1.9 \times 10^{-2} \times 1.9 \times 10^{-2}) \text{ m}^3$

2.5 Mesh convergence study

The three-dimensional thermal steady-state simulation was developed using ANSYS 17.2. The grid influence was also controlled by changing the element count from 540714 to 1081428, as shown in Figure 3. Because additional elements had no discernible effect on the temperature values, a fine mesh of 751611 elements was chosen.

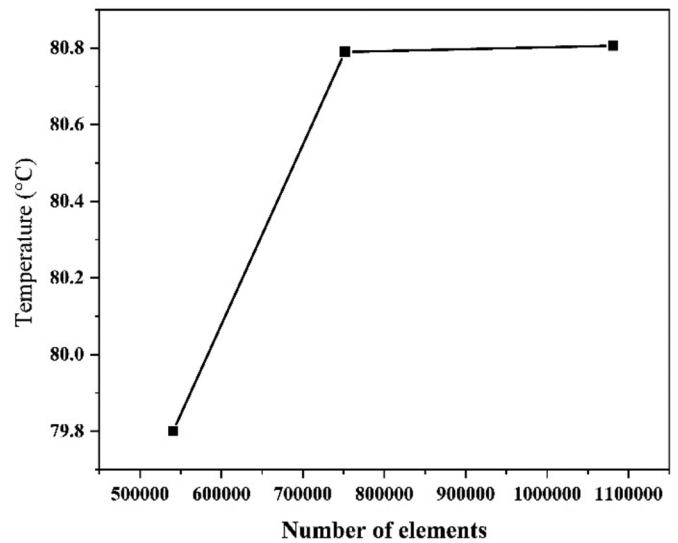


Fig. 3. Mesh convergence study.

2.6 Data reduction

To evaluate the LED case temperature, the temperature of interface material and heat sink thermal resistance, the following equations (2), (3) and (4) were used [16].

$$T_j = T_c + (R_{j-c} \times P_d) \quad (2)$$

$$T_b = T_c - (R_{TIM} \times P_d) \quad (3)$$

$$R_h = (T_b - T_a) / P_d \quad (4)$$

Where T_j , T_c , R_{j-c} , P_d , R_h , T_b , T_a and R_{TIM} denotes the LED junction temperature ($^\circ\text{C}$), LED case temperature ($^\circ\text{C}$), thermal resistance at the junction ($^\circ\text{C/W}$), dissipated

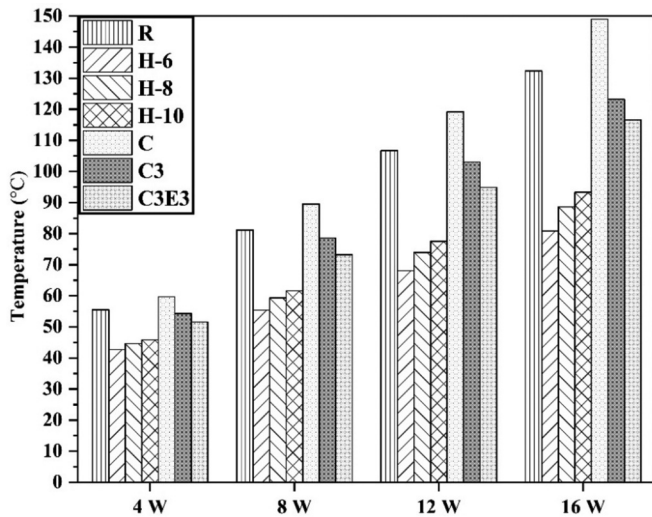


Fig. 4. Maximum temperature observed for different heat sink at varying power.

power (W), thermal resistance associated with the heat sink ($^{\circ}\text{C}/\text{W}$), the temperature of interface material ($^{\circ}\text{C}$), ambient temperature ($^{\circ}\text{C}$), and thermal interface. The thermal resistance of the material used in this study was extracted from the datasheet provided by the supplier.

3 Results and discussions

3.1 Temperature distribution

In this study, the steady-state thermal characterization on high power LEDs of different heat sink configurations was carried out. The thermal characteristics of the LED, i.e., the temperature distribution of different types of heat sinks, is presented in Figure 4. The results are obtained for different power levels, i.e., 4 W, 8 W, 12 W, and 16 W. The maximum temperature observed in the H-6 heat sink was 80.8°C at 16 W input power and 45.77% lower than the C heat sink. The H-6 heat sink was maintained at a lower temperature due to the more surface area and fins than other heat sink types. The maximum temperature of 55.59°C , 42.70°C , 44.66°C , 45.88°C , 59.70°C , 54.30°C and 51.64°C was recorded for heat sinks R, H-6, H-8, H-10, C, C-3 and C3E3, respectively, at an input power of 4 W. The H-6 heat sink exhibits better thermal performance than the other types of heat sinks. Similar results were obtained when input powers were 8 W and 12 W, respectively. The temperature contours for different heat sinks at 16 W are shown in Figure 5. The result revealed that the temperature distribution of the H-6 heat sink was 80.8°C at 16 W input power and 38.92% lower than that of the R heat sink. This significant cooling performance of the H-6 heat sink was due to more fins than the R heat sink. Figure 6 depicts the temperature distribution of the

H-6 heat sink against four different input power. The maximum temperature accumulated in the centre of the LED module is observed in Figure 6. The maximum temperature was observed for the H-6 heat sink at 16 W, compared to 4 W, because of the high heat density. The result showed the temperature of the H-6 heat sink was 68.10°C at 12 W input power which is 15.71% lower at 16 W input power. Therefore, it was concluded that the H-6 heat sink is the optimal design for high power LED lighting applications. The hot spots (maximum temperature in the LED module) were considered LED junction temperature (T_j).

3.2 Temperature distribution along the centre line of the heat sink

The temperature distribution along the centre line of the heat sink of the LED at 16 W, shown in Figure 7. The maximum temperatures at center of LED chip, were 132.3°C , 80.8°C , 88.6°C , 93.3°C , 149.0°C , 123.2°C and 116.6°C for R heat sink, H-6 heat sink, H-8 heat sink, H-10 heat sink, C heat sink, C3 heat sink and C3E3 respectively, at 16 W input power. The H-6 heat sink proved to be highly effective in keeping the chip temperature within the safe operating range, compare to other heat sinks. Because of its more surface area compare to other heat sinks.

3.3 Temperature of interface material

The interface material is vital in high power LED package. The reduction in the thermal resistance at the LED junction the lower operating temperature of the LED was recorded. The temperature of the interface material was calculated using equation (3). The lowest interface material temperature of 54.11°C was achieved by the H-6 heat sink when the input power was used at 16 W, as shown in Figure 8. The results observed that the interface material temperature of the H-6 heat sink was reduced by about 9%, compared with the H-8 heat sink at 16 W. This is due to the reduction of the LED junction temperature and thermal resistance of heat sinks. Hence the H-6 heat sink can help improve the performance of high-power LEDs.

3.4 Heat sink thermal resistance

The LED junction temperature was related to heat sink thermal resistance. The heat sink thermal resistance was calculated using equation (4). The influence of the number of fins on heat sink thermal resistance is illustrated in Figure 9. It can be observed that as the number of fins and surface areas increases, heat sink thermal resistance decreases. The heat sink thermal resistance is $5.89^{\circ}\text{C}/\text{W}$, $1.84^{\circ}\text{C}/\text{W}$, $2.46^{\circ}\text{C}/\text{W}$, $2.78^{\circ}\text{C}/\text{W}$, $7.13^{\circ}\text{C}/\text{W}$, $5.47^{\circ}\text{C}/\text{W}$, and $4.6^{\circ}\text{C}/\text{W}$ for R heat sink, H-6 heat sink, H-8 heat sink, H-10 heat sink, C heat sink, C3 heat sink, and C3E3 heat sink, respectively at 12W input power. Due to the LED's increased cooling thermal performance, the lifetime of LED will also increase.

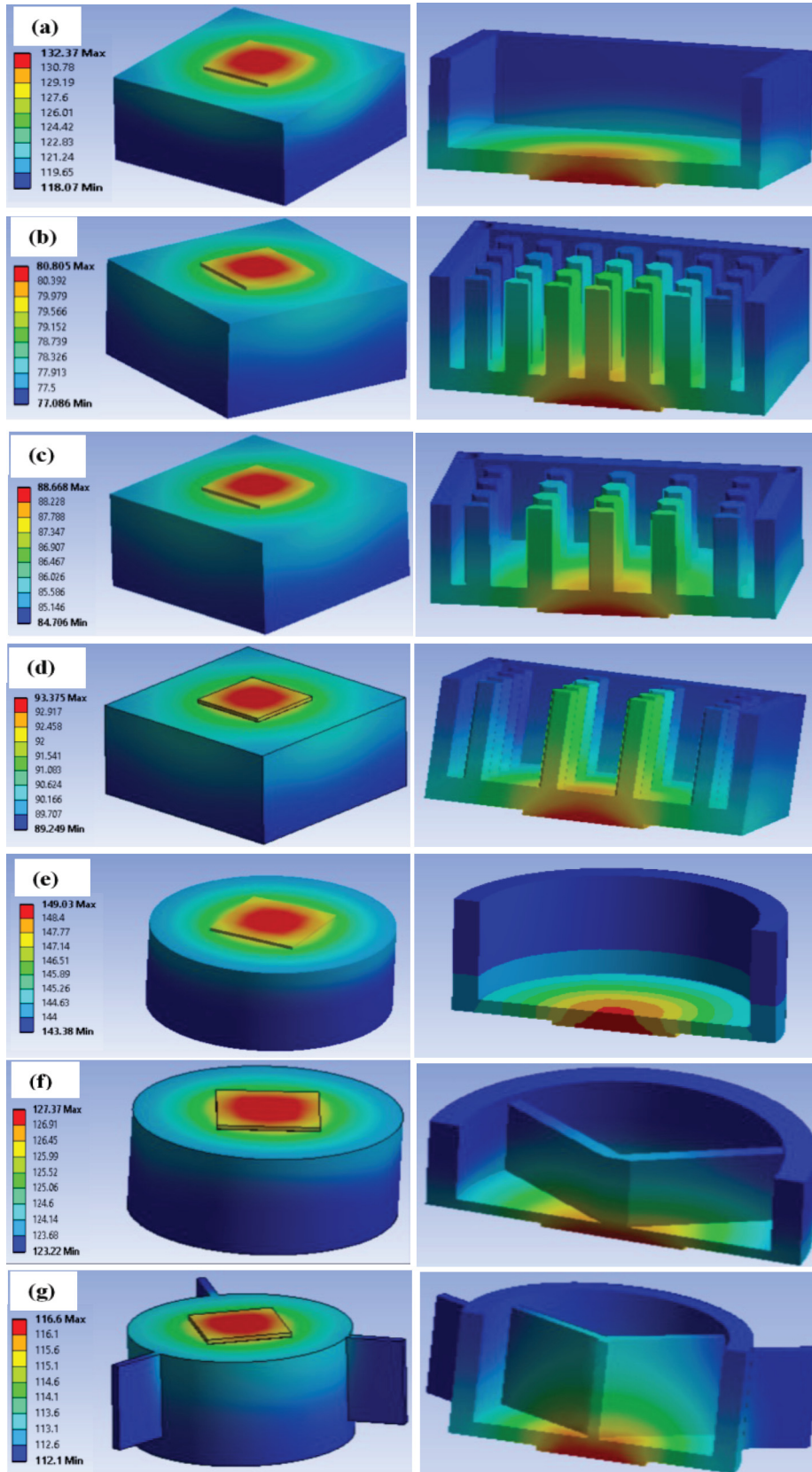


Fig. 5. Temperature contours for different heat sink with cross section at 16 W (a) R, (b) H-6, (c) H-8, (d) H-10, (e) C, (f) C3 and (g) C3E3.

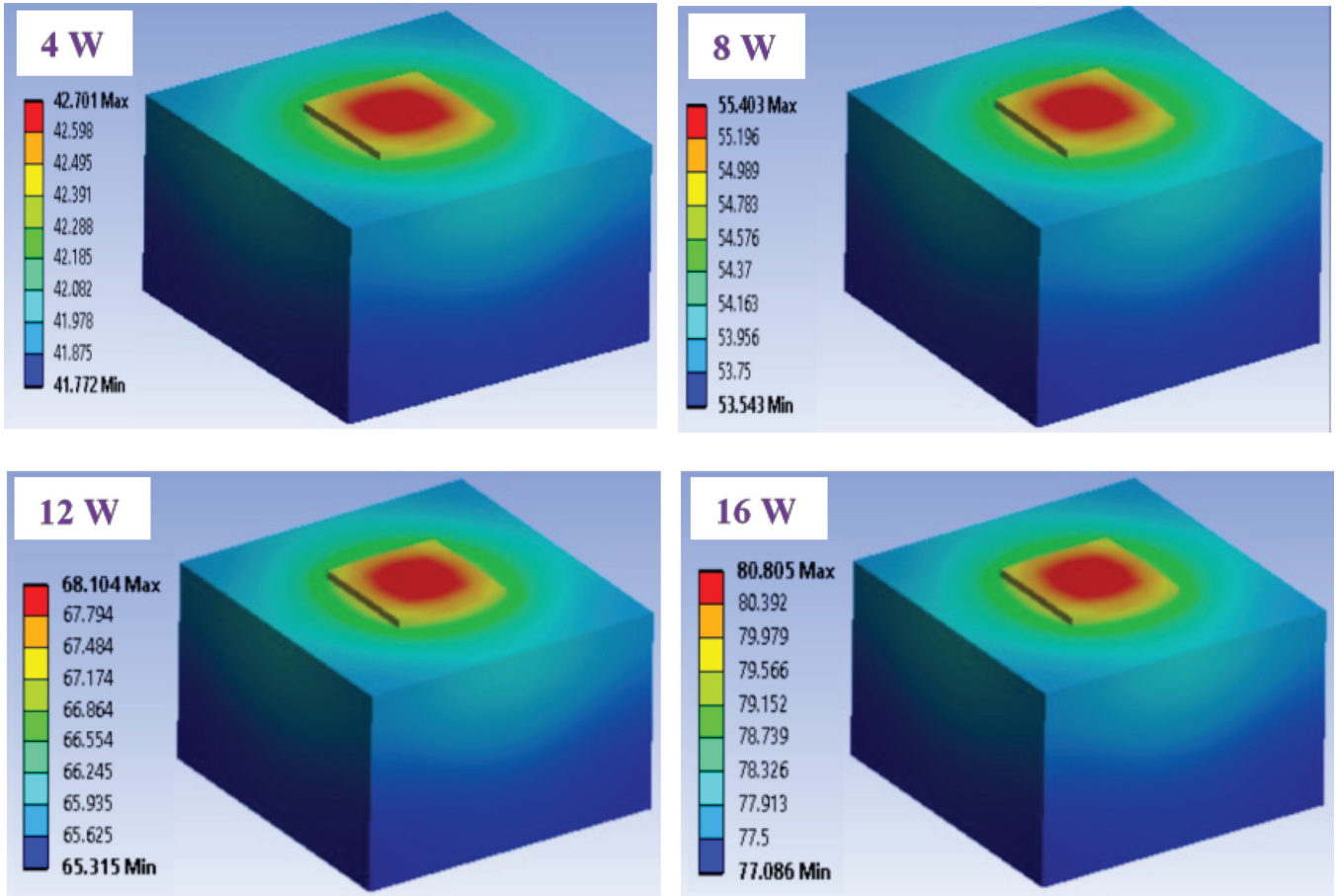


Fig. 6. Temperature contours for H-6 heat sink with different input power.

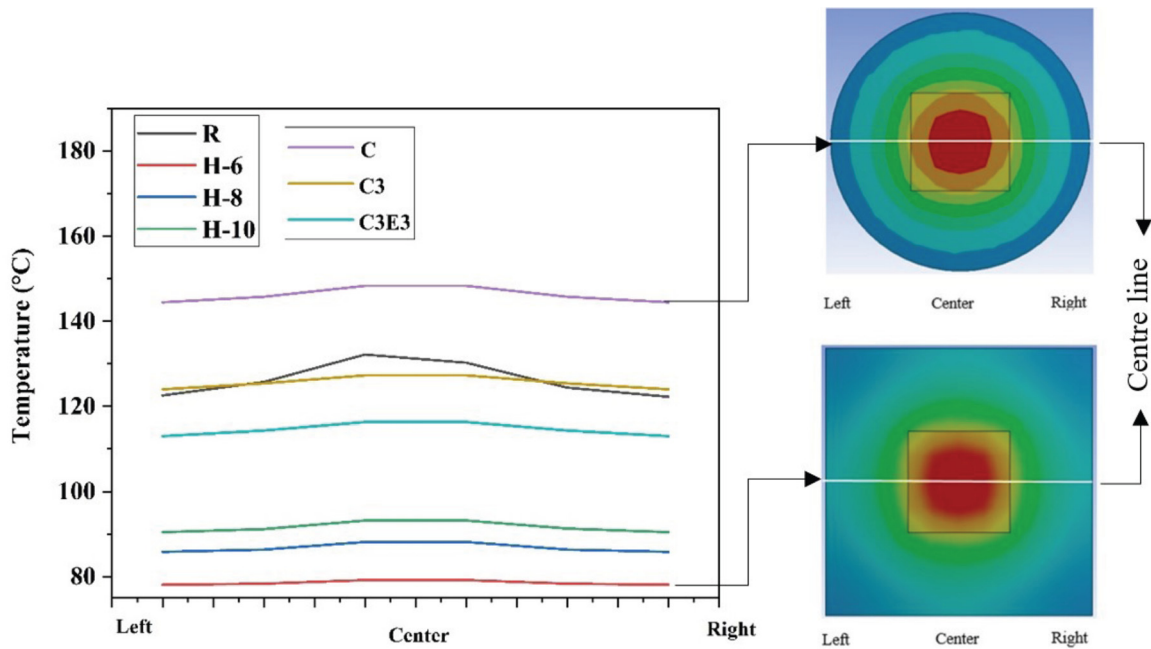


Fig. 7. Temperature distribution along the centre line of the heat sink.

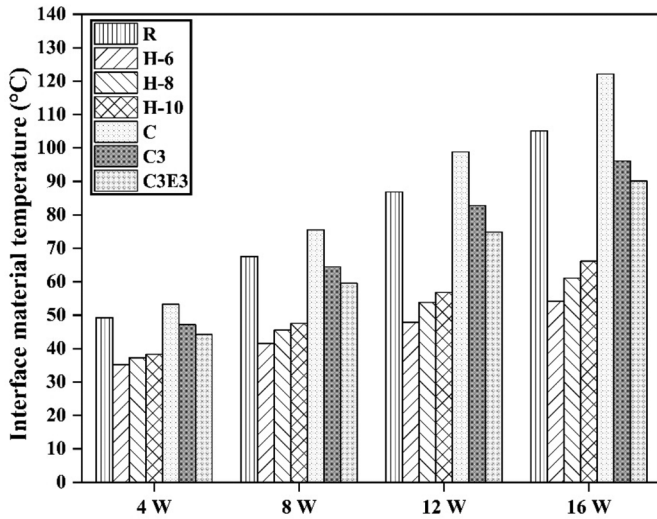


Fig. 8. Interface material temperature at different input power.

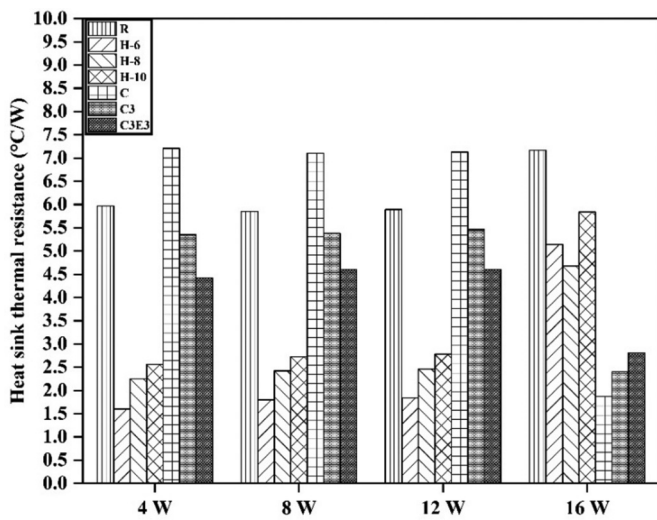


Fig. 9. Heat sink thermal resistance.

4 Conclusion

A simulation study was performed to estimate the maximum LED junction temperature with different heat sink models under steady-state thermal conditions. Based on the heat sink with hexagonal shape pin fins, heat sink plate fins were designed using a design tool. The simulation results reveal that the maximum temperature in the H-6 heat sink was about 45.78% lower than that of the C heat sink at 16 W input power. Furthermore, At 16 W input power, the heat sinks thermal resistance of the H-6 heat

sink reduced up to 73.91% compared with the C heat sink. The lowest interface material temperature of 54.11 °C was achieved by the H-6 heat sink when the input power was used 16 W. Increasing the number of heat sinks gives better thermal performance due to more surface area than without fin heat sink. The observed results encourage using more surface area-based heat sink suitable for high power LED thermal management.

References

1. P. Morgan, M. Hansen, J.Y. Tsao, LED lighting efficacy: status and directions, *Comptes Rendus Phys.* **1**, 1–12 (2017)
2. K. Ben Abdelmlek, Z. Araoud, L. Canale, K. Charrada, G. Zissis, Optimal substrate design for thermal management of high power multi-chip LEDs module, *Optik (Stuttg.)* **242**, 167179 (2021)
3. H.H. Cheng, D.S. Huang, M.T. Lin, Heat dissipation design and analysis of high power LED array using the finite element method, *Microelectron. Reliab.* **52**, 905–911 (2012)
4. F. He, Q. Chen, J. Liu, J. Liu, Thermal analysis of COB array soldered on heat sink, *Int. Commun. Heat Mass Transf.* **59**, 55–60 (2014)
5. X. Lin, S. Mo, L. Jia, Z. Yang, Y. Chen, Z. Cheng, Experimental study and Taguchi analysis on LED cooling by thermoelectric cooler integrated with microchannel heat sink, *Appl. Energy* **242**, 232–238 (2019)
6. X. Deng, Z. Luo, Z. Xia, W. Gong, L. Wang, Active-passive combined and closed-loop control for the thermal management of high-power LED based on a dual synthetic jet actuator, *Energy Convers. Manag.* **132**, 207–212 (2017)
7. S. Sundar, G. Song, M.Z. Zahir, J.S. Jayakumar, S.-J. Yook, Performance investigation of radial heat sink with circular base and perforated staggered fin, *Int. J. Heat Mass Transf.* **151**, 1–9 (2019)
8. D.S. Huang, T.C. Chen, L. Te Tsai, M.T. Lin, Design of fins with a grooved heat pipe for dissipation of heat from high-powered automotive LED headlights, *Energy Convers. Manag.* **180**, 550–558 (2019)
9. M. Wang, H. Tao, Z. Sun, C. Zhang, The development and performance of the high-power LED radiator, *Int. J. Therm. Sci.* **113**, 65–72 (2017)
10. Y. Huaiyu, S. Koh, H. Van Zeijl, A.W.J. Gielen, A review of passive thermal management of LED module, *J. Semicond.* **32**, 0140008–1: 014008–4 (2011)
11. S. Ragavanantham, S. Sampathkumar, S.S. Kumar, A study of temperature distribution and its effect on grinding wheel surface during wheel loading, *ASME 2016 Int. Mech. Eng. Congr. Expo.* **2**, 2–6 (2017)
12. D. Vinothraj, S. Ragavanantham, M. Saravanakumar, M. Vivekananthan, G.S. Sivagnanamani, Heat dissipation and inter-relationship between physical properties of moulding sand, *Mater. Today Proc.* **37**, 1809–1812 (2020)
13. B. Li, C. Byon, Orientation effects on thermal performance of radial heat sinks with a concentric ring subject to natural convection, *Int. J. Heat Mass Transf.* **90**, 102–108 (2015)
14. S. Feng, M. Shi, H. Yan, S. Sun, F. Li, J. Lu, Natural convection in a cross-fin heat sink, *Appl. Therm. Eng.* **132**, 30–37 (2017)

15. M.W. Jeong, S.W. Jeon, Y. Kim, Optimal thermal design of a horizontal fin heat sink with a modified-opening model mounted on an LED module, *Appl. Therm. Eng.* **91**, 105–115 (2015)
16. T. Ramesh, A.S. Praveen, P.B. Pillai, Phase change material aided thermal scheming of high power LED: effect of PCM with varying pitch of hexagonal fins, *Mater. Res. Innov.* **25**, 1–10 (2021)

Cite this article as: Thangamani Ramesh, Ayyappan Susila Praveen, Praveen Bhaskaran Pillai, Sachin Salunkhe, Numerical simulation of heat sinks with different configurations for high power LED thermal management, *Int. J. Simul. Multidisci. Des. Optim.* **13**, 18 (2022)